ISSN 1674-1056
http://cpb.iphy.ac.cn
http://iopscience.iop.org/cpb
中国物理 B
Chinese Physics
中国物理 Chinese Physics B

Stabilization of formamidinium lead iodide perovskite precursor solution for blade-coating efficient carbon electrode perovskite solar cells

Yu Zhan(占宇), Weijie Chen(陈炜杰), Fu Yang(杨甫), and Yaowen Li(李耀文)
Citation: Chin. Phys. B, 2021, 30 (**8**): 088803. DOI: 10.1088/1674-1056/abfbcb
Journal homepage: http://cpb.iphy.ac.cn; http://iopscience.iop.org/cpb

What follows is a list of articles you may be interested in

Influence of CdS films synthesized by different methods on the photovoltaic performance of CdTe/CdS thin film solar cells

Jun Wang(汪俊), Yuquan Wang(王玉全), Cong Liu(刘聪), Meiling Sun(孙美玲), Cao Wang(王操), Guangchao Yin(尹广超), Fuchao Jia(贾福超), Yannan Mu(牟艳男), Xiaolin Liu(刘笑林), Haibin Yang(杨海滨)
Chin. Phys. B, 2020, 29 (**9**): 098802. DOI: 10.1088/1674-1056/abad22

Current improvement in substrate structured Sb_2S_3 solar cells with $MoSe_2$ interlayer

Lu Liu(刘璐), Sheng-Li Zhang(张生利), Jian-Yu Wu(吴建宇), Wei-Huang Wang(王伟煌), Wei Liu(刘玮), Li Wu(武莉), Yi Zhang(张毅)
Chin. Phys. B, 2020, 29 (**5**): 058801. DOI: 10.1088/1674-1056/ab8220

Two-step processed efficient perovskite solar cells via improving perovskite/PTAA interface using solvent engineering in PbI_2 precursor

Cao-Yu Long(龙操玉), Ning Wang(王宁), Ke-Qing Huang(黄可卿), Heng-Yue Li(李恒月), Biao Liu(刘标), Jun-Liang Yang(阳军亮)
Chin. Phys. B, 2020, 29 (**4**): 048801. DOI: 10.1088/1674-1056/ab7744

Designing solar-cell absorber materials through computational high-throughput screening

Xiaowei Jiang(江小蔚), Wan-Jian Yin(尹万健)
Chin. Phys. B, 2020, 29 (**2**): 028803. DOI: 10.1088/1674-1056/ab6655

The effect of Mn-doped ZnSe passivation layer on the performance of CdS/CdSe quantum dot-sensitized solar cells

Yun-Long Deng(邓云龙), Zhi-Yuan Xu(徐知源), Kai Cai(蔡凯), Fei Ma(马飞), Juan Hou(侯娟), Shang-Long Peng(彭尚龙)
Chin. Phys. B, 2019, 28 (**9**): 098802. DOI: 10.1088/1674-1056/ab37f3

RAPID COMMUNICATION

Stabilization of formamidinium lead iodide perovskite precursor solution for blade-coating efficient carbon electrode perovskite solar cells*

Yu Zhan(占宇), Weijie Chen(陈炜杰), Fu Yang(杨甫)†, and Yaowen Li(李耀文)‡

Laboratory of Advanced Optoelectronic Materials, College of Chemistry, Chemical Engineering and Materials Science, Soochow University, Suzhou 215123, *China*

(Received 31 March 2021; revised manuscript received 24 April 2021; accepted manuscript online 27 April 2021)

Formamidinium lead triiodide ($FAPbI_3$) is a research hotspot in perovskite photovoltaics due to its broad light absorption and proper thermal stability. However, quite a few researches focused on the stability of the $FAPbI_3$ perovskite precursor solutions. Besides, the most efficient $FAPbI_3$ layers are prepared by the spin-coating method, which is limited to the size of the device. Herein, the stability of $FAPbI_3$ perovskite solution with methylammonium chloride (MACl) or cesium chloride (CsCl) additive is studied for preparing perovskite film through an upscalable blade-coating method. Each additive works well for achieving a high-quality $FAPbI_3$ film, resulting in efficient carbon electrode perovskite solar cells (pero-SCs) in the ambient condition. However, the perovskite solution with MACl additive shows poor aging stability that no α-$FAPbI_3$ phase is observed when the solution is aged over one week. While the perovskite solution with CsCl additive shows promising aging stability that it still forms high-quality pure α-$FAPbI_3$ perovskite film even the solution is aged over one month. During the solution aging process, the MACl could be decomposed into methylamine which will form some unfavored intermediated phase inducing δ-phase $FAPbI_3$. Whereas, replacing MACl with CsCl could effectively solve this issue. Our founding shows that there is a great need to develop a non-MACl $FAPbI_3$ perovskite precursor solution for cost-effective preparation of pero-SCs.

Keywords: perovskite precursor solution, formamidinium lead iodide, blade-coating, carbon electrode

PACS: 88.40.H–, 88.40.hj, 84.60.Jt **DOI:** 10.1088/1674-1056/abfbcb

1. Introduction

Formamidinium lead triiodide ($FAPbI_3$) has a lower bandgap of $\sim$ 1.45 eV, which affords a broader solar light absorption and better thermal stability with respect to methylammonium lead triiodide ($MAPbI_3$).[1,2] In 2019, a certified power conversion efficiency (PCE) of 23.7% was obtained by Seok *et al.*, along with a high short-circuit density (J_{sc}) up to 26.7 mA/cm.[3] Recently, the certified PCE of $FAPbI_3$ pero-SCs has been increased up to 25.2%, with a J_{sc} of 26.25 mA/cm^2, a V_{oc} of 1.174 V, and a fill factor (FF) of 81.8%, which indicates its promising potential for the commercialization of $FAPbI_3$ photovoltaic devices.[4] However, spontaneous conversion of the desired trigonal black α-phase into the undesired wide-bandgap δ-phase with hexagonal symmetry under ambient conditions at room temperature poses a serious challenge for its practical applications.[5] To enhance the phase stability of $FAPbI_3$ perovskite, many researchers incorporated $MAPbBr_3$ into the perovskite to form $(FAPbI_3)_{1-x}(MAPbBr_3)_x$ perovskite films, which give lots of start-of-art results.[5–10] In addition, incorporating methylammonium chloride (MACl) into the $FAPbI_3$ perovskite precursor solution is widely used to induce an intermediate to the pure α-phase $FAPbI_3$, along with the improved morphology of the perovskite film.[3,4,11,12] However, it has been reported that it can easily form the δ-phase $FAPbI_3$ over the aging time of the FA perovskite precursor solution with MA^+ cations, which will directly affect its photovoltaic performance.[13] Therefore, the long-term stability of the perovskite precursor solution needs to be considered in the preparation of cost-efficient perovskite devices for the future application of perovskite photovoltaics.

On the other hand, most of $FAPbI_3$ pero-SCs with the impressive PCE results have been fabricated by spin-coating, which is limited to film area, wastes most of the solution, and not compatible with the upscaling process.[14–17] Blade-coating is the most frequently employed process next to spin coating in lab-scale experiments for fabricating films of well-defined thickness.[18–20] It can serve as a lab-scale analogue to the slot die coating process which could be applied on a roll to roll and sheet to sheet manufacturing process. However, most perovskite films fabricated by the blade-coating method are

*Project supported by the Key Research and Development Program of China (Grant No. 2020YFB1506400), the National Natural Science Foundation of China (Grant Nos. 51922074, 51673138, 51820105003, and 22075194), the Tang Scholar, the Priority Academic Program Development of Jiangsu Higher Education Institutions (PAPD), and Collaborative Innovation Center of Suzhou Nano Science and Technology.

†Corresponding author. E-mail: fuyang@suda.edu.cn

‡Corresponding author. E-mail: ywli@suda.edu.cn

© 2021 Chinese Physical Society and IOP Publishing Ltd

MA only or MA–FA mixed perovskites which usually have the risk in the long-term stability for the devices because of the low thermal and light instability of MA.[18,19,21–28] Besides, most researches in blade-coating pero-SCs only fabricate the perovskite films by blade-coating method, and still use spin-coating and evaporation methods for preparing the charge transport layers and top electrode, which is limited for the upscaling process and consume a lot of energy. Therefore, fully blade-coating the high-quality MA-free pero-SCs with thermal stability and moisture resistance is highly desired for perfect PSCs, which is challenging but urgently required. Owing to the high electrical conductivity, low cost, easy fabrication, upscalable, and chemical stability, carbon electrode has great potential in the application on efficient and stable perovskite solar cells.[29,30]

In this paper, through optimizing MACl additive content in the perovskite precursor solution to improve the film quality and avoid the δ-phase $FAPbI_3$, pure α-phase $FAPbI_3$ perovskite film with grain size over 2 μm was successfully prepared by the gas-quenching assisted blade-coating method in the ambient air condition. Through blade-coating the electron transport layer, perovskite layer, hole transport layer, the carbon as the top electrode, PCE over 15% was achieved in this planar carbon electrode perovskite solar cells. However, the MACl additive perovskite solution was unstable which resulted in a high δ-phase $FAPbI_3$ content in the perovskite film when kept the caped solution at ambient atmosphere for 1 week. Those results were confirmed by x-ray diffraction (XRD) and ultraviolet-visible (UV-vis) spectra. On the other hand, replacing MACl with cesium chloride (CsCl) also worked well for increasing the film quality and obtaining the pure α-phase $FAPbI_3$ perovskite film through the blade-coating method. Besides, the perovskite solution with CsCl additive is highly stable and it still can form high-quality α-phase $FAPbI_3$ perovskite film even it is aged over one month. The reason for the low stability MACl additive perovskite precursor solution is that the decompose of MA^+ to methylamine could induce the δ-phase $FAPbI_3$.

2. Results and discussion

2.1. $FAPbI_3$ perovskite film analysis

The effects of different content of MACl and CsCl as the additive in $FAPbI_3$ perovskite precursor solution on the morphology of the $FAPbI_3$ perovskite film were studied by using field emission scanning electron microscopy (FE-SEM). Figure 1 shows that all the perovskite films are pin-hole free films and the grain size is gradually increased when increasing the MACl or CsCl content in the perovskite precursor solution. At last, the grain size could be over 2 μm when over 20% MACl or 10% CsCl was incorporated. The grain size is one of the governing parameters for determining the diffusion length and the charge carrier recombination rate of the perovskite layer.[31–33] A large number of grain boundaries are presented in the perovskite layer with small grain size, which will not only act as charge trap sites, but also prone to attack by water molecules which will accelerate the degradation of the perovskite.[34] Figure S5 shows the relative strain as a function of CsCl content. The relative strain was calculated by the Williamson–Hall plot using a linear fitting. A reduced strain was found for the perovskite film with 10% CsCl. Further increasing CsCl content over 10% led to increased strain.

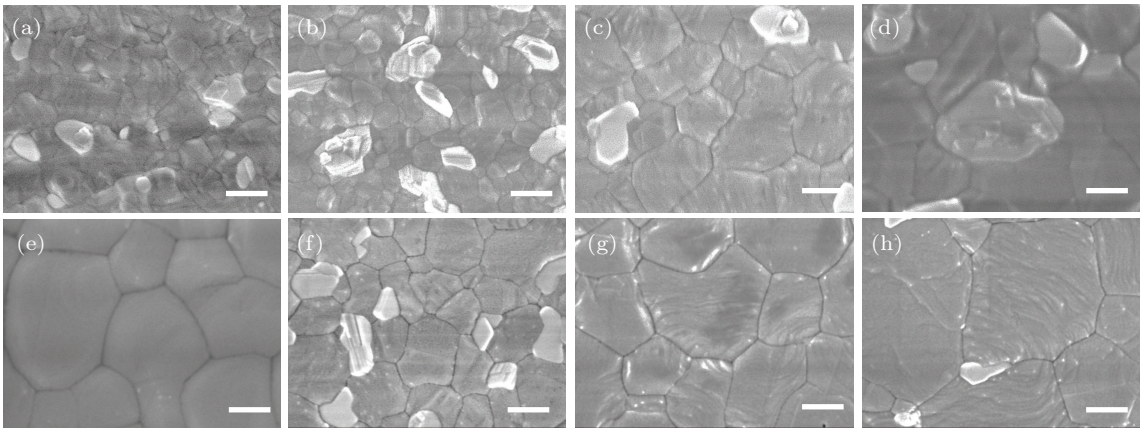


Fig. 1. Top-view SEM images of annealed $FAPbI_3$ perovskite films prepared by gas-quenching assisted blade-coating of precursor solutions with different molar ratios of MACl or CsCl. (a) Control, (b) 10% mol MACl, (c) 20% mol MACl, (d) 30% mol MACl, (e) 40% mol MACl, (f) 5% mol CsCl, (g) 10% mol CsCl, (h) 15% mol. CsCl. Scale bars are 1 μm.

Then, the $FAPbI_3$ film quality derived from the different conditions of MACl and CsCl additive was explored by XRD spectra and UV-vis spectra shown in Fig. 2. Upon inducing MACl and CsCl additive, two typical peaks at 14.3° and 28.6° were observed which are assigned to the (001) and (002) crystal planes of α-$FAPbI_3$. Besides, the characteristic peak of the non-perovskite δ-$FAPbI_3$ phase was found at 11.8° in the pristine perovskite film. While the δ-$FAPbI_3$ phase disappears when intruding MACl or CsCl into the perovskite precursor solution. Upon increasing the content of MACl or CsCl ad-

ditive inside the perovskite precursor solution, the intensity of peaks for the α-$FAPbI_3$ phase is greatly improved, which is in agreement with the SEM results. Further, the lead iodide peak located at 12.7° is also decreased when increasing the ratio of the MACl and CsCl additive, which will be a benefit for the stability of the perovskites film as the degradation rate of the perovskite film could be accelerated because of the PbI_2 residue present in the perovskite film. The UV-vis spectra shown in Figs. 2(c) and 2(d) exhibit a greatly enhanced absorption when inducing MACl or CsCl as the additive, indicating an improved film quality, which can be attributed to better surface coverage and improved crystallinity. However, when increasing the content of CsCl additive over 10% mol, the absorption edge shifts to a lower wavelength, which indicates that the bandgap of perovskite becomes wider due to the incorporation of Cs into the perovskite crystal lattice.

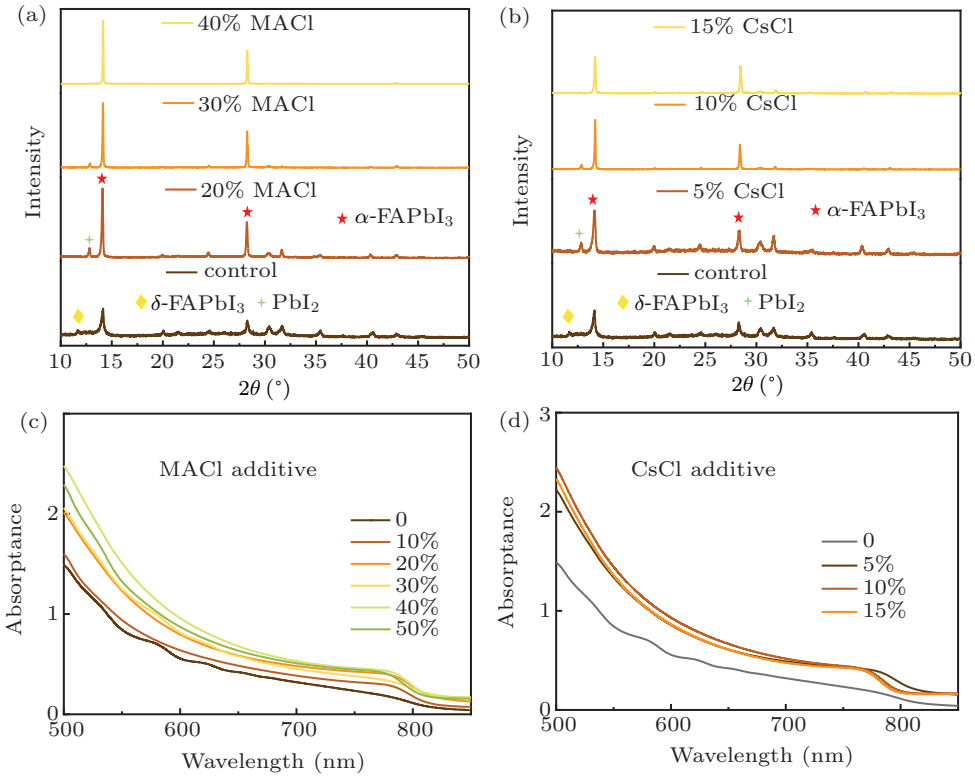


Fig. 2. Effect of the addition of different concentrations of MACl or CsCl to the precursor solution of $FAPbI_3$ on the properties of the final $FAPbI_3$ perovskite film. XRD spectra of (a) MACl, (b) CsCl. UV-vis spectra of (c) MACl, (d) CsCl.

2.2. Device performance

To check the effect of the perovskite film derived from the different additive conditions, pero-SCs with the architecture of ITO/SnO_2/perovskite/poly(3-hexylthiophene) (P3HT)/carbon were fabricated and the photovoltaic statistical results are shown in Fig. 3. The current density is slightly increased when increasing the MACl additive ratio from 10% mol to 40% mol, while it is decreased when the ratio is 50% mol, resulting in the highest J_{sc} of 22.6 ± 0.3 mA/cm^2 at the case of 40% mol MACl. V_{oc} is increased from 986.7 ± 11.4 mV of the control to 1027.7 ± 13.1 mV of the 10% mol MACl, 1034.3 ± 11.7 mV of the 20% mol MACl, 1060.4 ± 15.5 mV of the 30% mol MACl, 1076.3 ± 9.6 mV of the 40% mol MACl, and 1110.6 ± 10.7 mV of the 50% mol MACl. The FF shows a similar trend as that of the current density with the best FF of $63.5 \pm 1.7\%$ for the case of 40% mol MACl. As a result, the best PCE of $15.5 \pm 0.6\%$ is obtained for the case of 40% mol MACl additive. In addition, the performance trend of the CsCl additive is similar to that of MACl with the best performance achieved for the case of 10% mol CsCl with an average J_{sc} of 22.1 ± 0.5 mA/cm^2, V_{oc} of 1064 ± 18.3 mV, FF of $60.5 \pm 1.2\%$, PCE of $14.3 \pm 0.4\%$. Figure S1 shows the J–V curves of the PSCs derived from the perovskite solution with different content of additive. In conclusion, both additive cases work well for improving the performance of $FAPbI_3$ perovskite devices.

2.3. Stability of perovskite solution

The stability of the perovskite precursor solution was explored by checking the solution with 40% mol MACl or 10% mol CsCl respectively. The precursor solution was aged at ambient air condition with a relative humidity of 30–40% R.H. for different time. Then the aged solution was blade coated for preparing the perovskite film and solar cells. Figure 4 shows the XRD results of the perovskite film derived from the aged solution. Strong non-perovskite δ-$FAPbI_3$ phase at 11.8° is shown in Fig. 4(a) when aging the case of 40% mol MACl additive over one week. Meanwhile, the typi-

cal peaks at 14.3° and 28.6° almost disappear, indicating no α-$FAPbI_3$ exists in the perovskite film. There is no black color from the photograph of the perovskite film which agrees with the XRD results. On the other hand, for the case of 10% mol CsCl, the α-$FAPbI_3$ peaks at 14.3° and 28.6° are almost not changed even the perovskite solution aging over one month along with no non-perovskite δ-FAPbI3 phase at 11.8° shown in the film, indicating high stability of the perovskite solution of the CsCl additive case. Figure S2 shows the $FAPbI_3$ perovskite derived from different content of MACl (0, 10% mol, 20% mol, 30% mol, 40% mol, 50% mol) additive in the $FAPbI_3$ perovskite precursor solution aged for one week. Upon increasing the MACl content, the perovskite solution became worse over one week aging, which indicates the poor stability of the MACl additive $FAPbI_3$ perovskite precursor solution, which also conforms from the XRD results from Fig. S3. While the perovskite solution with different content of CsCl (0, 5% mol, 10% mol, 15% mol) additive is highly stable which can be proved by the XRD results in Fig. S4. The stability of $FAPbI_3$ perovskite solution without additive also works well which can be illustrated in the following XRD result of the perovskite film derived from the $FAPbI_3$ perovskite pristine solution aged for a different time (Fig. S6). However, it needs to mention that the film quality would become worse without additive which resulted in less efficient perovskite solar cells shown in Fig. 3.

Pero-SCs based on the above perovskite film were prepared and the results are shown in Fig. 5. Performance of the devices derived the aged 40% MACl additive in $FAPbI_3$ perovskite solution decreases rapidly to $4.9 \pm 0.4\%$ mainly due to the decreased J_{sc} and FF. However, there is just a slight drop of the performance of the devices derived from the aged 10% CsCl additive perovskite solution with a stable J_{sc}. Those results are in accordance with the XRD results shown in Fig. 4, which clearly proves the long-term stability of the CsCl additive $FAPbI_3$ precursor solution.

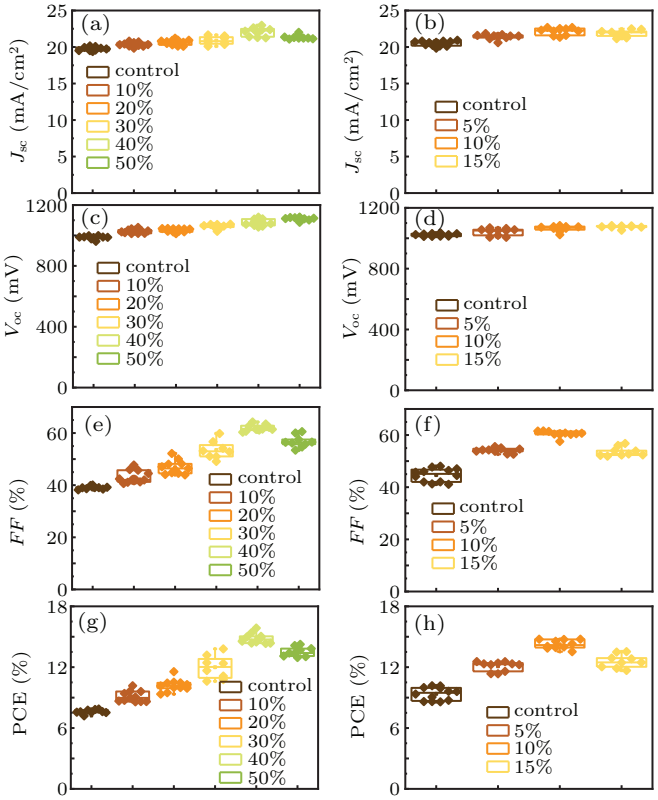


Fig. 3. Photovoltaic statistics for the fully printed planar PSCs with the structure of ITO/SnO_2/perovskite/P3HT/carbon for different amounts of MACl or CsCl additive. (a) J_{sc}, (c) V_{oc}, (e) FF, and (g) PCE for MACl additive. (b) J_{sc}, (d) V_{oc}, (f) FF, and (h) PCE for CsCl additive.

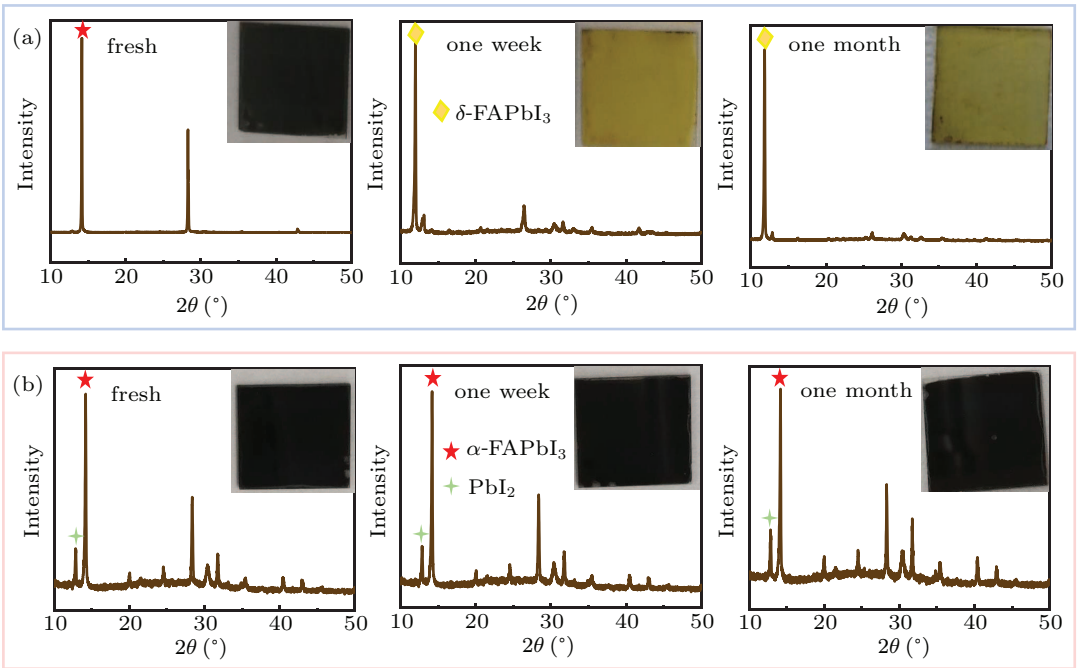


Fig. 4. XRD patterns of films deposited from a precursor solution aged for different times. (a) 40% mol MACl, (b) 10% mol CsCl additive.

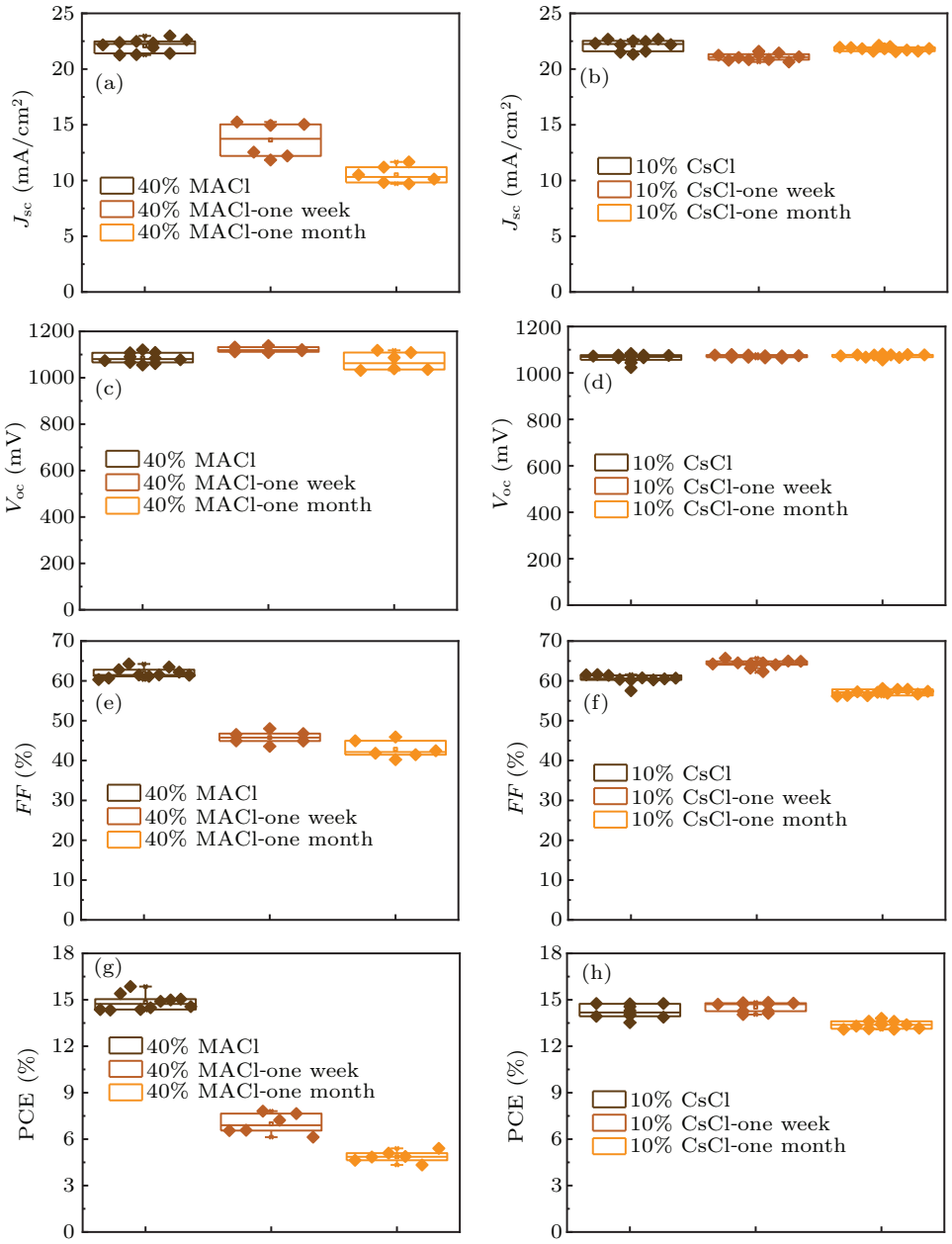


Fig. 5. Photovoltaic statistics for the fully printed planar PSCs with the structure of ITO/SnO_2/perovskite/P3HT/carbon, 40% mol MACl or 10% mol CsCl added into the precursor solution aged for different time. (a) J_{sc}, (c) V_{oc}, (e) FF, and (g) PCE for MACl additive. (b) J_{sc}, (d) V_{oc}, (f) FF, and (h) efficiency for CsCl additive.

2.4. Mechanism explanation

Next, the proposed mechanism for the low-stability of MACl additive $FAPbI_3$ perovskite solution is explored and proposed as

$$CH_3NH_3Cl \rightarrow CH_3NH_2 + HCl,$$
$$FAI + PbI_2 \xrightarrow{CH_3NH_2} \delta - FAPbI_3.$$

Methylammonium chloride will decompose to methylamine during the aging of MACl additive $FAPbI_3$ perovskite precursor solution, which will form some intermediate phase inducing the non-perovskite δ-$FAPbI_3$ phase.[13] This i could be proved by the UV-vis absorbance spectra shown in Figs. 6(a) and 6(b), which indicates that there is a clear difference in the intermediate state as the absorbance discrepancy of the non-annealed perovskite film derived from the aged one-month MACl or CsCl additive perovskite solution. Besides, UV-vis absorbance spectra shown in Figs. 6(b) and 6(c) clearly exhibit that there is a significant difference in a range from the wavelength of 450 nm to 700 nm for the non-annealed perovskite film derived from the aged one-month MACl or CsCl additive perovskite solution, indicating that the intermediate state is greatly affected by the MACl decomposition. This will directly induce the non-perovskite δ-$FAPbI_3$ phase, which is also proved by Pang *et al.*[13] This non-perovskite δ-$FAPbI_3$ phenomenon can exclude the effect of Cl from the MACl as CsCl additive solution worked well in the aged solution. The above results show the great potential of the non-MACl perovskite precursor solution for the cost-effective preparation of perovskite solar cells.

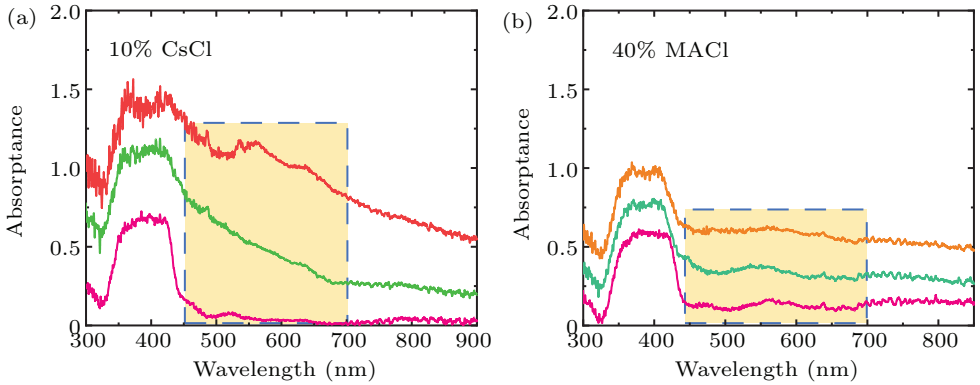


Fig. 6. UV-vis spectra of the perovskite wet film prepared for different time under the preparing condition (pink curve: just coated and before gas quenching, green curve: during gas quenching, red curve: just after gas quenching). Films deposited from the over one-month aged precursor solution with 40% mol MACl (a) or 10% mol CsCl (b).

3. Conclusion

We have successfully optimized MACl, CsCl as an additive into the $FAPbI_3$ perovskite precursor solution to improve the film quality and avoid the δ-phase $FAPbI_3$ by the gas-quenching assisted blade-coating method in the ambient air condition. Besides, SnO_2, the perovskite layer, P3HT, and the carbon electrode were blade-coated for preparing a fully printable device with PCE over 15%. However, the MACl additive perovskite solution is unstable which resulted in a high δ-phase $FAPbI_3$ content in the perovskite film even kept the caped solution at ambient atmosphere for 1 day. On the other hand, replacing MACl with CsCl as the additive leads a highly stable precursor solution which can still provide pure α-phase $FAPbI_3$ perovskite even those films are prepared by the over one-month aged perovskite precursor solution. The reason for the low stability MACl additive perovskite precursor solution is that the decompose of MA^+ to methylamine could form an unfavored intermediate phase, inducing the δ-phase $FAPbI_3$. The above results show the great potential of the non-MACl $FAPbI_3$ perovskite precursor solution for cost-effective preparation of perovskite solar cells.

References

[1] Eperon G E, Stranks S D, Menelaou C, Johnston M B, Herz L M and Snaith H J 2014 *Energy Environ. Sci.* **7** 982

[2] Diao X, Tang Y and Xie Q 2019 *Chin. Phys. B* **28** 17802

[3] Min H, Kim M, Lee S U, Kim H, Kim G, Choi K, Lee J H and Seok S I 2019 *Science* **366** 749

[4] Jeong J, Kim M, Seo J, Lu H, Ahlawat P, Mishra A, Yang Y, Hope M A, Eickemeyer F T, Kim M, Yoon Y J, Choi I W, Darwich B P, Choi S J, Jo Y, Lee J H, Walker B, Zakeeruddin S M, Emsley L, Rothlisberger U, Hagfeldt A, Kim D S, Grätzel M and Kim J Y 2021 *Nature* **592** 381

[5] Jeon N J, Noh J H, Yang W S, Kim Y C, Ryu S, Seo J and Seok S I 2015 *Nature* **517** 476

[6] Yang W S, Noh J H, Jeon N J, Kim Y C, Ryu S, Seo J and Seok S I 2015 *Science* **348** 1234

[7] Jiang Q, Zhao Y, Zhang X, Yang X, Chen Y, Chu Z, Ye Q, Li X, Yin Z and You J 2019 *Nat. Photon.* **13** 460

[8] Jiang Q, Zhang L, Wang H, Yang X, Meng J, Liu H, Yin Z, Wu J, Zhang X and You J 2016 *Nat. Energy* **2** 16177

[9] Zhou H, Chen Q, Li G, Luo S, Song T B, Duan H S, Hong Z, You J, Liu Y and Yang Y 2014 *Science* **345** 542

[10] Xu G, Xue R, Stuard S J, Ade H, Zhang C, Yao J, Li Y and Li Y 2021 *Adv. Mater.* **33** 2006753

[11] Yang F, Dong L, Jang D, Tam K C, Zhang K, Li N, Guo F, Li C, Arrive C, Bertrand M, Brabec C J and Egelhaaf H J 2020 *Adv. Energy Mater.* **10** 2001869

[12] Hui W, Chao L, Lu H, Xia F, Wei Q, Su Z, Niu T, Tao L, Du B, Li D, Wang Y, Dong H, Zuo S, Li B, Shi W, Ran X, Li P, Zhang H, Wu Z, Ran C, Song L, Xing G, Gao X, Zhang J, Xia Y, Chen Y and Huang W 2021 *Science* **371** 1359

[13] Wang X, Fan Y, Wang L, Chen C, Li Z, Liu R, Meng H, Shao Z, Du X, Zhang H, Cui G and Pang S 2020 *Chem* **6** 1369

[14] Bruening K, Dou B, Simonaitis J, Lin Y Y, van Hest M F and Tassone C J 2018 *Joule* **2** 2464

[15] Li Z, Klein T R, Kim D H, Yang M, Berry J J, van Hest M F and Zhu K 2018 *Nat. Rev. Mater.* **3** 1

[16] Cai M, Wu Y, Chen H, Yang X, Qiang Y and Han L 2017 *Adv. Sci.* **4** 1600269

[17] Qiu L, He S, Ono L K, Liu S and Qi Y 2019 *ACS Energy Lett.* **4** 2147

[18] Guo F, He W, Qiu S, Wang C, Liu X, Forberich K, Brabec C J and Mai Y 2019 *Adv. Funct. Mater.* **29** 1900964

[19] Guo F, Qiu S, Hu J, Wang H, Cai B, Li J, Yuan X, Liu X, Forberich K and Brabec C J 2019 *Adv. Sci.* **6** 1901067

[20] Xue R, Zhang M, Luo D, Chen W, Zhu R, Yang M, Li Y and Li Y 2020 *Sci. China Chem.* **63** 987

[21] Yang F, Kamarudin M A, Hirotani D, Zhang P, Kapil G, Ng C H, Ma T and Hayase S 2019 *Sol. RRL* **3** 1800275

[22] Yang F, Zhang P, Kamarudin M A, Kapil G, Ma T and Hayase S 2018 *Adv. Funct. Mater.* **28** 1804856

[23] Dou B, Whitaker J B, Bruening K, Moore D T, Wheeler L M, Ryter J, Breslin N J, Berry J J, Garner S M and Barnes F S 2018 *ACS Energy Lett.* **3** 2558

[24] Hu H, Ren Z, Fong P W, Qin M, Liu D, Lei D, Lu X and Li G 2019 *Adv. Funct. Mater.* **29** 1900092

[25] Deng Y, Zheng X, Bai Y, Wang Q, Zhao J and Huang J 2018 *Nat. Energy* **3** 560

[26] Dai X, Deng Y, Van Brackle C H, Chen S, Rudd P N, Xiao X, Lin Y, Chen B and Huang J 2020 *Adv. Energy Mater.* **10** 1903108

[27] Deng Y, Van Brackle C H, Dai X, Zhao J, Chen B and Huang J 2019 *Sci. Adv.* **5** eaax7537

[28] Wu W Q, Yang Z, Rudd P N, Shao Y, Dai X, Wei H, Zhao J, Fang Y, Wang Q and Liu Y 2019 *Sci. Adv.* **5** eaav8925

[29] Fagiolari L and Bella F 2019 *Energy Environ. Sci.* **12** 3437

[30] Gao L, Zhou Y, Meng F, Li Y, Liu A, Li Y, Zhang C, Fan M, Wei G and Ma T 2020 *Carbon* **162** 267

[31] Yang F, Kamarudin M A, Kapil G, Hirotani D, Zhang P, Ng C H, Ma T and Hayase S 2018 *ACS Appl. Mater. Interfaces* **10** 24543

[32] Nie W, Tsai H, Asadpour R, Blancon J C, Neukirch A J, Gupta G, Crochet J J, Chhowalla M, Tretiak S, Alam M A, Wang H L and Mohite A D 2015 *Science* **347** 522

[33] Kim H D, Ohkita H, Benten H and Ito S 2016 *Adv. Mater.* **28** 917

[34] Castro-Méndez A F, Hidalgo J and Correa-Baena J P 2019 *Adv. Energy Mater.* **9** 1901489